Surface Thermal Boundary Condition for Ocean Circulation Models

ROBERT L. HANEY

Dept. of Meteorology, Naval Postgraduate School, Monterey, Calif.

(Manuscript received 1 March 1971, in revised form 7 June 1971)

ABSTRACT

By employing a heat budget analysis appropriate to zonally and time averaged conditions within the atmosphere, it is shown that the net downward heat flux Q at the ocean's surface can be expressed as $Q=Q_2(T_A^*-T_S)$, where T_A^* is an apparent atmospheric equilibrium temperature, T_S the sea surface temperature, and Q_2 a coefficient determined from the zonally and time averaged data. The latter coefficient, which is of the order of 70 ly day^{-1} (°C)$^{-1}$, varies with latitude by as much as 20%. It is suggested that the use of the above relation as a flux-type thermal boundary condition would allow for large-scale thermal coupling of ocean and atmosphere. The more common use of specified T_S as a boundary condition clearly does not allow for such coupling.

1. Introduction

Until the pioneering joint work of Manabe (1969) and Bryan (1969), numerical studies treated the atmospheric and oceanic circulations separately, with the energy input either parameterized or specified. In atmospheric general circulation models (Mintz, 1964; Manabe *et al.*, 1965; Kasahara and Washington, 1967), the lower boundary condition in the heat equation over the ocean involves a specification of the ocean surface temperature. The upward flux of longwave radiation, sensible and latent heat are then calculated as a function of the prescribed ocean surface temperature and such dependent variables as the air temperature, relative humidity and surface wind speed.

In ocean circulation models (Bryan and Cox, 1967, 1968; Cox, 1970), the general procedure is to prescribe the ocean surface temperature and then calculate the downward heat flux using the same value of κ as is used for the vertical eddy diffusion of heat in the ocean depths. For example, if T_S is the prescribed ocean surface temperature, and T_1 is the temperature at the first level below the surface, then the downward heat flux Q is calculated from

$$\frac{Q}{\rho_0 c}=\kappa\frac{\partial T}{\partial z}=\frac{\kappa}{\Delta z}(T_S-T_1), \tag{1}$$

where ρ_0 is the density of sea water, c the specific heat of sea water at constant pressure, Δz the depth of the first layer, and κ the vertical eddy diffusion coefficient for heat (see Fig. 1).

The primary weakness in formulating the heat flux according to (1) is an insufficient knowledge of the appropriate value of κ to be used in the surface layer. It is usually considered that it should be somewhat larger there than in the thermocline or deeper layers, but no quantitative determination has been made. In the present work, we formulate a boundary condition on the ocean surface temperature which gives the heat flux into the ocean independently of κ. The method is somewhat similar to one used by Charney (1959) in an atmospheric model.

2. Formulation of the heat flux components

The basic assumption for this formulation is that the ocean is in contact with an atmospheric equilibrium state which is constant in time. The particular atmospheric state and the particular method by which the ocean exchanges heat with the atmosphere are also important. We start by writing the total downward flux of heat across the ocean surface as the sum of the downward flux of solar radiation Q_S, minus the net upward flux of longwave (or "back") radiation Q_B, sensible heat Q_H, and latent heat Q_E. If the net downward heat flux is denoted by Q, we have

$$Q=Q_S-(Q_B+Q_H+Q_E). \tag{2}$$

a. Solar radiation

The downward flux of solar radiation which penetrates the ocean surface, Q_S, is given by the amount of insolation which strikes the sea surface (ground), Q_G, reduced by the albedo of the ocean surface,[1] α_G, i.e.,

$$Q_S=Q_G(1-\alpha_G). \tag{3}$$

The amount of solar radiation which strikes the ocean surface, Q_G, is given by that which is incident on a horizontal surface at the top of the atmosphere, Q_0, reduced by the albedo of clouds, α_C, the albedo of a

[1] The reflection coefficient α_G is for the combined direct and diffuse radiation; the solar radiation is not further subdivided since we are concerned with zonally and time averaged quantities.

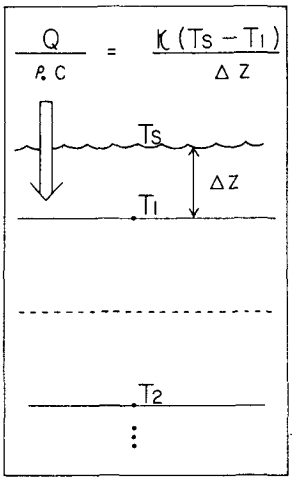

FIG. 1. Schematic diagram depicting the formulation of downward heat flux at the ocean surface according to (1). In this formulation, the ocean surface temperature T_S is prescribed.

cloudless atmosphere due to air molecules and dust and water vapor scattering, α_A, and the absorptivity of the atmosphere, A_A; thus, we have

$$Q_G = Q_0[1-(\alpha_C+\alpha_A+A_A)]. \tag{4}$$

Substituting (4) into (3), we have the downward flux of solar radiation into the ocean

$$Q_S = Q_0[1-(\alpha_C+\alpha_A+A_A)](1-\alpha_G). \tag{5}$$

Using (5), Q_S was calculated as a function of latitude from 50S to 50N using zonally averaged annual mean data as follows. The absorptivity A_A and the albedo α_A of a cloudless atmosphere were taken to be the constant values 0.18 and 0.08, respectively (London, 1957). The albedo α_G of the ocean surface was taken to be the slowly increasing function of latitude shown by the dashed curve in Fig. 2 (Katayama, 1966). The cloud albedo α_C was calculated from the new planetary albedo measurements of Vonder Haar and Hanson (1969) as follows. From the definition of the planetary albedo α_p as the ratio of the upward scattered (or reflected) energy which reaches the top of the atmosphere to the incoming isolation at the top of the atmosphere, we may write

$$\begin{aligned}\alpha_p &\equiv (Q_{RA}+Q_{RC}+Q_{RG})/Q_0 \\ &= \alpha_A+\alpha_C+\alpha_G Q_G/Q_0,\end{aligned} \tag{6}$$

where Q_{RA}, Q_{RC} and Q_{RG} is the amount of solar radiation scattered or reflected to space by the atmosphere, by clouds and by the ocean surface, respectively, and the albedos are defined by

$$\left.\begin{aligned}\alpha_A &\equiv Q_{RA}/Q_0 \\ \alpha_C &\equiv Q_{RC}/Q_0 \\ \alpha_G &\equiv Q_{RG}/Q_G\end{aligned}\right\}. \tag{7}$$

Substituting Q_G/Q_0 from (4) into (6) and solving for α_C, we have

$$\alpha_C = \{[\alpha_p-\alpha_G(1-A_A)]/(1-\alpha_G)\}-\alpha_A. \tag{8}$$

Using the values of α_G, α_A and A_A noted above, and the values of the planetary albedo α_p given by Vonder Haar and Hanson (1969), α_C was calculated as a function of latitude from 50S to 50N using (8). The solid curve in Fig. 2 shows the sum of α_C and the constants α_A and A_A. The zonal mean solar radiation at the top of the atmosphere, Q_0, was taken to be that reported by London (1957) based on a solar constant of 2 ly min^{-1}, and is shown by the solid curve in Fig. 3.

At best, (8) is a rather rough approximation to the albedo of clouds. It is that value of the total cloud albedo which is required (along with reasonably well-known values of α_A, α_G and A_A) to produce the mean planetary albedo pattern, α_p, determined by the satellite measurements of Vonder Haar and Hanson (1969). It should be pointed out that the value of α_C so determined is really only used in calculating the long-wave radiation [see (14) below] because (5) may be

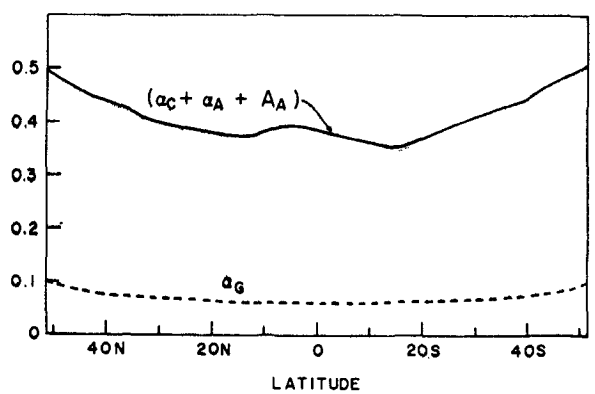

FIG. 2. Latitudinal variation of the sum of the albedo due to clouds, the albedo due to dust and haze, and the absorptivity of the atmosphere (solid curve) and albedo of the ocean surface (dashed curve).

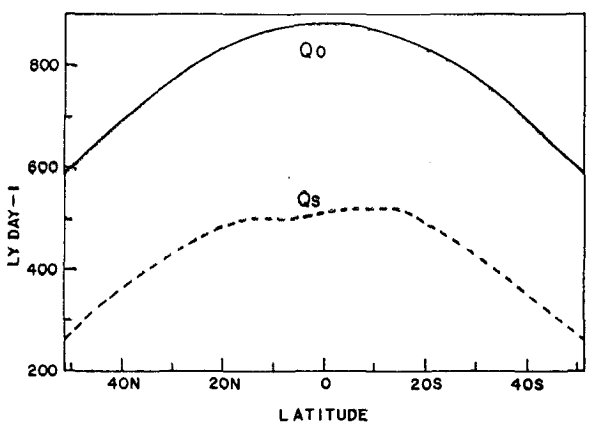

FIG. 3. Latitudinal variation of the solar radiation at the top of the atmosphere (solid curve) and the solar radiation absorbed at the ocean surface (dashed curve).

written solely in terms of Q_0, α_p and A_A as

$$Q_S = Q_0[1-(\alpha_p+A_A)].$$

Using the above values of Q_0, $(\alpha_C+\alpha_A+A_A)$ and α_G, Q_S was calculated from (5) as a function of latitude from 50S to 50N and is shown by the dashed curve in Fig. 3. The resulting values of Q_S are larger than earlier estimates because of Vonder Haar and Hanson's smaller planetary albedo. Vonder Haar and Hanson explain that previous calculations of α_p which used conventional cloud data overestimated the reflectivity of clouds, especially that of high clouds.

b. Net longwave radiation

The net upward flux of longwave radiation, Q_B, is approximated by the following empirical relationship due to Brunt (1952), which was also used by Kraus and Rooth (1961):

$$Q_B(T_S) = Q^*\sigma T_S^4, \tag{9}$$

where

$$Q^* = 0.985[0.39-0.05(e_A)^{\frac{1}{2}}](1-0.6n_C^2), \tag{10}$$

and σ is the Stefan-Boltzmann constant, T_S the ocean surface temperature (°K), e_A the vapor pressure (mb) of the air 10 m above sea level, and n_C the fractional cloud cover. The dependence of Q^* on the vapor pressure and the cloud cover parameterizes the reduction of upward longwave radiation by water vapor and clouds in the atmosphere (often referred to inaccurately as the "greenhouse effect"). Unlike the shortwave radiation Q_S, the net upward flux of longwave radiation, Q_B, depends upon the ocean surface temperature T_S. Based on Budyko's Saviño-Ångström formula (Malkus, 1962), we assume that the albedo due to clouds is related linearly to the cloud fraction n_C, so that the cloud fraction can be calculated from the previously obtained values of cloud albedo (8) as

$$n_C = \alpha_C/0.6. \tag{11}$$

The vapor pressure e_A can be expressed in terms of the saturation vapor pressure e_S at the temperature of the air T_A (10 m above sea level) and the ratio $r \equiv e_A/e_S(T_A)$, which is the relative humidity in decimal form; that is,

$$e_A \equiv re_S(T_A), \tag{12}$$

where the saturation vapor pressure $e_S(T)$ is given by the following integrated form of the Clausius-Clapeyron equation (Fleagle and Businger, 1963):

$$e_S(T) = 10^{(9.4051-2353/T)}. \tag{13}$$

Using (11) and (12), we can write (10) as

$$Q^* = 0.985\{0.39-0.05[re_S(T_A)]^{\frac{1}{2}}\} \times[1-0.6(\alpha_C/0.6)^2], \tag{14}$$

where $e_S(T_A)$ is given by (13).

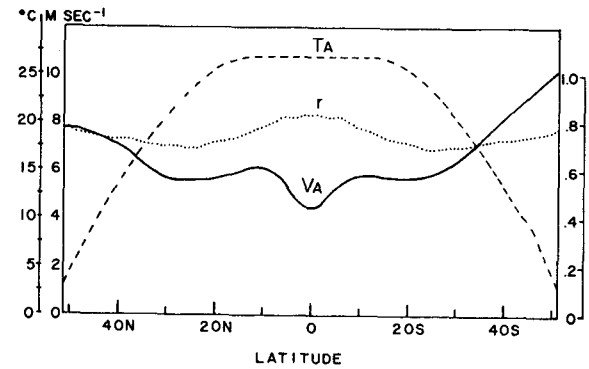

FIG. 4. Latitudinal variation of the surface air temperature T_A(°C), the relative humidity ratio r, and the surface wind speed V_A(m sec^{-1}). See text for data sources.

If we assume that the air-sea temperature difference is small, we may expand the functional dependence of Q_B on T_S in a truncated Taylor series about the temperature T_A; thus, we have

$$Q_B(T_S) = Q_B(T_A) + \left(\frac{\partial Q_B}{\partial T}\right)_{T_A}(T_S-T_A). \tag{15}$$

Substituting (9) into (15), we have

$$Q_B(T_S) = Q^*\sigma T_A^4 + 4Q^*\sigma T_A^3(T_S-T_A), \tag{16}$$

where Q^* is given by (14). According to (16), $4Q^*\sigma T_A^3$ gives the net upward flux of longwave radiation per degree Celsius by which the ocean surface temperature T_S exceeds the atmospheric equilibrium temperature T_A.

The zonally averaged annual mean surface air temperature T_A and relative humidity ratio r from London (1957) are shown in Fig. 4. Using these data and the cloud albedo calculated from (8), the quantities $Q^*\sigma T_A^4$ and $4Q^*\sigma T_A^3$ were determined as functions of latitude from 50S to 50N and are shown in Fig. 5. The smallness of $4Q^*\sigma T_A^3$ [<5 ly day^{-1} (°C)$^{-1}$] indicates that variations in net back radiation due to variations in the ocean surface temperature are extremely small.

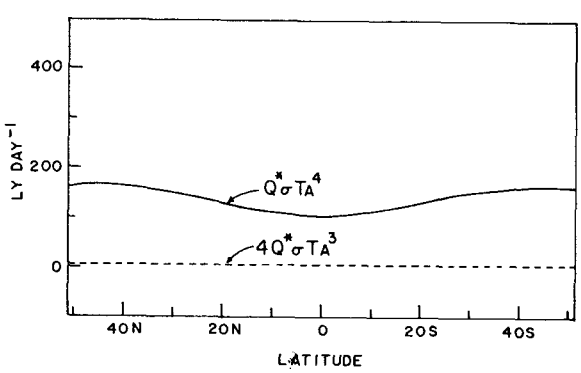

FIG. 5. Latitudinal variation of the quantities $Q^*\sigma T_A^4$ (ly day^{-1}) and $4Q^*\sigma T_A^3$ [ly day^{-1} (°C)$^{-1}$] which enter into the calculation of the longwave radiation $Q_B(T_S)$ in (16).

Our calculation indicates that the net back radiation at the temperature T_A, $Q^*\sigma T_A^4$, has a maximum near 40° latitude, whereas Katayama (1967) shows the net back radiation to have a maximum near 20°. By using mean annual surface temperature and relative humidity data, our calculation probably does not properly account for the large decrease of downward longwave radiation in the latitude belt of the dry subtropical highs. However, this discrepancy is not significant for the purpose of this investigation.

c. Sensible and latent heat flux

The vertical flux of sensible and latent heat is parameterized by the turbulent transfer formulas. Over the tropical oceans, where turbulent shear flow is the major process governing the transports, such a parameterization is well founded. However, the use of climatological data in the transfer formulas for sensible and latent heat is not so easily justified. This is not only because of the variability of atmospheric conditions due to synoptic disturbances and the nonlinearity of the transfer formulas, but also because the values of the transfer coefficients have been determined from synoptic rather than climatological data. The importance of synoptic disturbances in the air-sea energy exchange has been well demonstrated by Garstang (1967) who showed that the total heat transfer from the ocean to the atmosphere in low latitudes is about twice as large during the passage of synoptic-scale disturbances as during undisturbed periods. It is therefore recognized that calculations based on climatological data can be expected to give only approximate results. However, as long as we work within the framework of an ocean circulation model which is forced by a *stationary* atmospheric state, we have no other choice. A possible next step would be to allow the atmospheric state to change with time in a way which simulates the variation of all of the atmospheric parameters during steady passages of synoptic disturbances and during the changing seasons. Indeed, the present method of formulating the heat flux across the ocean surface for a numerical ocean model was developed because of the ease with which the method can be generalized to such a more realistic form.

With the above limitations in mind, we write the upward flux of sensible and latent heat in terms of T_S and the prescribed atmospheric parameters as

$$\left.\begin{aligned} Q_H(T_S)&=\rho_A C_D V_A C_p(T_S-T_A)\\ Q_E(T_S)&=\rho_A C_D V_A L[q_S(T_S)-q_A]\end{aligned}\right\}, \tag{17}$$

where ρ_A is the air density, C_p the specific heat of air at constant pressure, C_D the drag coefficient, V_A the wind speed at anemometer level, L the latent heat of vaporization, $q_S(T_S)$ the saturation specific humidity at the temperature of the ocean surface T_S, and q_A the specific humidity of the air at anemometer level. Expanding $Q_E(T_S)$ in a truncated Taylor series about the temperature T_A, we have [similar to (15)]

$$Q_E(T_S)=Q_E(T_A)+\left(\frac{\partial Q_E}{\partial T}\right)_{T_A}(T_S-T_A). \tag{18}$$

Since $q_A/q_S(T_A)\approx e_A/e_S(T_A)\equiv r$, we can write from (17),

$$Q_E(T_A)=\rho_A C_D V_A L q_S(T_A)(1-r). \tag{19}$$

From (17),

$$\left(\frac{\partial Q_E}{\partial T}\right)_{T_A}=\rho_A C_D V_A L\left(\frac{\partial q_S}{\partial T}\right)_{T_A}. \tag{20}$$

If we substitute (13) into the relationship

$$q_S(T)=\frac{0.622}{p}e_S(T), \tag{21}$$

and then differentiate with respect to T, we have

$$\frac{\partial q_S}{\partial T}=\frac{0.622}{p}[(2353\ \ln 10)e_S(T)/T^2], \tag{22}$$

where p is the pressure in the same units as $e_S(T)$. Thus, (20) becomes

$$\left(\frac{\partial Q_E}{\partial T}\right)_{T_A}=\rho_A C_D V_A L\left(\frac{0.622}{p_A}\right)\times[(2353\ \ln 10)e_S(T_A)/T_A^2]. \tag{23}$$

Substituting (23) and (19) into (18), we have

$$Q_E(T_S)=Q_{E1}+Q_{E2}(T_S-T_A), \tag{24}$$

where

$$\left.\begin{aligned} Q_{E1}&=\rho_A C_D V_A L\left(\frac{0.622}{p_A}\right)e_S(T_A)(1-r)\\ Q_{E2}&=\rho_A C_D V_A L\left(\frac{0.622}{p_A}\right)[(2353\ \ln 10)e_S(T_A)/T_A^2]\end{aligned}\right\}. \tag{25}$$

In a manner analogous to (24), we may write

$$Q_H(T_S)=Q_{H1}+Q_{H2}(T_S-T_A), \tag{26}$$

where, from (17)

$$\left.\begin{aligned} Q_{H1}&=0\\ Q_{H2}&=\rho_A C_D V_A C_p\end{aligned}\right\}. \tag{27}$$

The quantities Q_{E1}, Q_{E2} and Q_{H2} were calculated from (25), (27) and (13) using the zonally averaged annual mean values of the surface wind speed V_A taken from the climatic charts of U. S. Weather Bureau (1938) along with T_A and r from Fig. 4. Also, the following

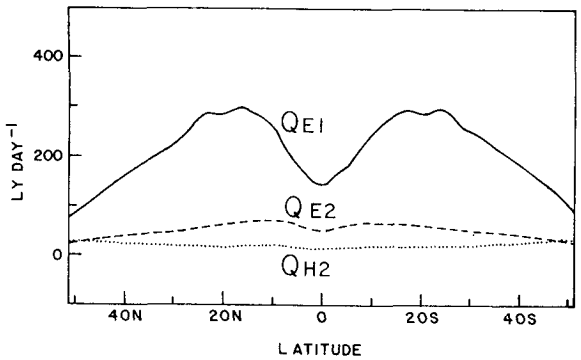

FIG. 6. Latitudinal variation of the quantities Q_{E1} (ly day^{-1}), Q_{E2} [ly day^{-1} (°C)$^{-1}$], and Q_{H2} [ly day^{-1} (°C)$^{-1}$] which control the sensible and latent heat flux. The values were computed from (25) and (27) using the constant drag coefficient, $C_D=1.4\times10^{-3}$.

constant values were used

$$\left.\begin{aligned} \rho_A &= 1.2\times10^{-3}\ \text{gm cm}^{-3} \\ L &= 595\ \text{cal gm}^{-1} \\ c_p &= 0.24\ \text{cal gm}^{-1}\ (°\text{C})^{-1} \\ p_A &= 1013.25\ \text{mb} \end{aligned}\right\}. \tag{28}$$

Two separate calculations were made, one using a constant drag coefficient (Riehl and Malkus, 1958; Weiler and Burling, 1967)

$$C_D=1.4\times10^{-3}, \tag{29}$$

and one using the variable drag coefficient proposed by Deacon and Webb (1962) for neutral stability, namely

$$C_D=(1.0+0.07V_A)\times10^{-3}, \tag{30}$$

where V_A is in meters per second. No attempt has been made to allow C_D to depend upon the static stability of the lower air, nor to incorporate the effects of a thin laminar boundary region close to the sea surface in which molecular diffusion dominates the vertical exchange of heat and moisture (Sheppard, 1958). The effect of such a laminar region is to increase C_D for heat and moisture at low wind speeds, and decrease it at high wind speeds, making C_D less dependent on the wind speed. For the present calculations, however, the use of the rather slowly increasing function of V_A given in (30) seems adequate for a comparison with (29). It is because of this uncertainty in the appropriate value of C_D that two calculations were made. The values of Q_{E1}, Q_{E2}, and Q_{H2} which were obtained using (29) and (30) are shown in Figs. 6 and 7, respectively. Since all of the data used to calculate Q_{E1}, Q_{E2} and Q_{H2} is zonally averaged annual mean data, the results shown in these figures can be considered approximations to zonal mean values. At the equator, where V_A is small and r large, the evaporative cooling, Q_{E1}, is a minimum, while in the adjacent trade-wind zones it is a maximum. Since the value of $C_D=1.4\times10^{-3}$ corresponds to a wind speed of 5.8 m sec^{-1} in (30), the main difference between the results shown in Figs. 6 and 7 occurs poleward of

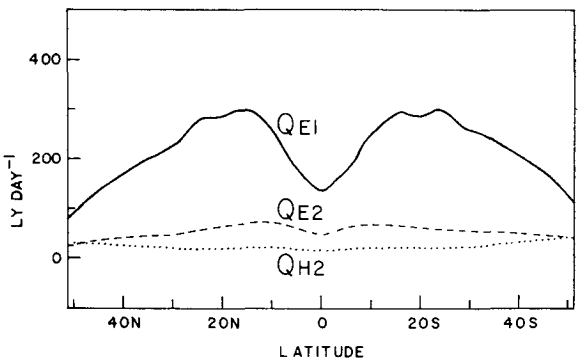

FIG. 7. Same as Fig. 6 except that C_D was taken from (30).

30° latitude in both hemispheres where V_A is considerably larger than 5.8 m sec^{-1} (Fig. 4). Therefore, in the middle latitudes of both hemispheres we have larger values of Q_{E1} and Q_{E2} when the variable C_D from (30) is used.

If we substitute (5), (16), (24) and (26) into (2), we can write the total downward heat flux across the ocean surface as

$$Q=Q_1+Q_2(T_A-T_S), \tag{31}$$

where

$$Q_1=Q_0[1-(\alpha_C+\alpha_A+A_A)](1-\alpha_G) -(Q^*\sigma T_A{}^4+Q_{E1}), \tag{32}$$

$$Q_2=4Q^*\sigma T_A{}^3+Q_{E2}+Q_{H2}. \tag{33}$$

The quantity Q_1 contains the net downward flux of solar radiation across the ocean surface, minus the upward flux of longwave radiation and latent heat from an ocean surface at temperature T_A; Q_2 contains the net upward flux of longwave radiation and sensible and latent heat per degree Celsius excess of ocean surface temperature over the atmospheric equilibrium temperature T_A. Fig. 8 shows Q_1 and Q_2 calculated from (32) and (33) with $C_D=1.4\times10^{-3}$, while Fig. 9 shows the results using the variable C_D given by (30). At the equator, where the evaporative cooling is at a minimum,

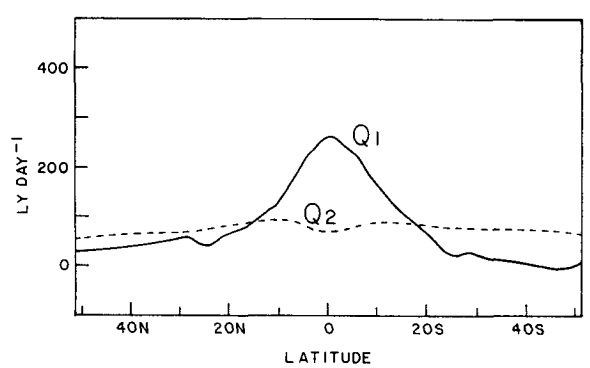

FIG. 8. Latitudinal variation of the quantities Q_1 (ly day^{-1}) and Q_2 [ly day^{-1} (°C)$^{-1}$] which control the downward heat flux Q. The values were computed from (32) and (33) with the constant coefficient $C_D=1.4\times10^{-3}$.

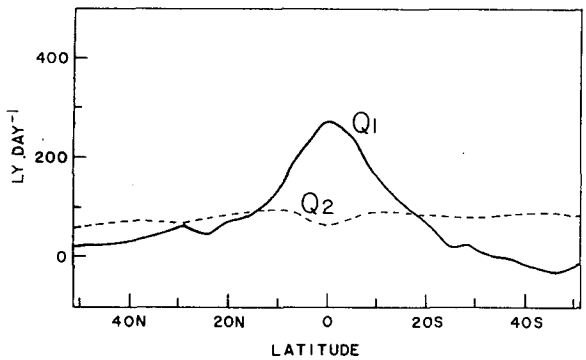

FIG. 9. Same as Fig. 8 except that C_D was taken from (30).

Q_1 has a rather sharp maximum in both formulations of the drag coefficient. The use of $C_D=1.4\times10^{-3}$ (Fig. 8) decreases the evaporative cooling in middle latitudes of the Southern Hemisphere where $V_A>5.8$ m sec^{-1}, thereby increasing Q_1 there. In both formulations of C_D, Q_2 varies between 60 and 95 ly day^{-1} (°C)$^{-1}$. However, south of 30S, Q_2 is about 25% larger than it is north of 30N, and this difference is greater in the case of the variable C_D.

In order to roughly judge the consistancy of the above results, (31) was used along with the annual mean observed ocean surface temperatures to calculate Q as a function of latitude for the North Pacific Ocean. The annual mean of the ocean surface temperatures at 180° longitude [reported in U. S. Naval Oceanographic Office (1969)] was used for T_S and the calculated Q is shown in Fig. 10. The dotted line shows the value of Q calculated from (31) using the constant C_D from (29); the dashed line is the result using the variable C_D from (30), while the solid line shows the annual mean Q at 180° obtained by Emig (1967) using the heat balance method and the data of Budyko *et al.* (1962). There appears to be rough qualitative agreement between the calculated and observed values. The values of Q calculated from (31) show net downward heat flux into the ocean south of 15N and net upward heat flux out of the ocean north of 15N (except at 45N where T_A may likely be erroneously large by 1 or 2C).

Another view of the consistency between the present results and estimates of the observed net heat flux across the ocean surface is obtained as follows. Because of the smallness of $4Q^*\sigma T_A^3$ (Fig. 5), the total upward transfer of sensible and latent heat calculated from (31) is approximately $Q_{E1}+Q_2(T_S-T_A)$. Using $Q_{E1}=300$ ly day^{-1} and $Q_2=90$ ly day^{-1} (°C)$^{-1}$ (typical near 15° latitude in Figs. 6 or 7, and 8 or 9), a sea-air temperature difference of 0.5–1.0C gives a total upward transfer of sensible and latent heat of

$$Q_{E1}+Q_2(T_S-T_A)\approx 345\text{–}390 \text{ ly day}^{-1}.$$

This is comparable to a mean annual value of about 350–500 ly day^{-1} estimated by Garstang (1967) for the tropical region near 15N over the Atlantic Ocean (his Figs. 11 and 12). The generally smaller value obtained in the present calculation from (31) is primarily due to the omission of a bulk Richardson number as a parameter to influence the drag coefficient.

3. Interpretations and conclusions

Another way of interpreting the heat flux formulation (31) is obtained by writing it in the form

$$Q=Q_2(T_A^*-T_S), \tag{34}$$

where

$$T_A^*=T_A+Q_1/Q_2 \tag{35}$$

is a kind of apparent atmospheric equilibrium temperature. Fig. 11 shows T_A and T_A^* calculated from (35) using the constant drag coefficient $C_D=1.4\times10^{-3}$. The important feature in this profile of T_A^* is that while T_A is constant in the equatorial region, T_A^* shows a distinct maximum at the equator. When T_A^* is calculated

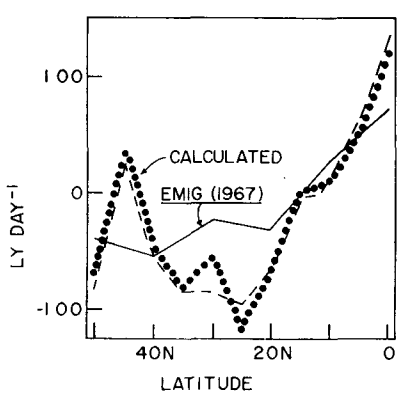

FIG. 10. The total heat flux Q calculated from (31) using observed ocean surface temperatures T_S, compared with the value of Q from Emig (1967). The dotted line shows the result using the constant C_D from (29) while the dashed line shows the result using the variable C_D from (30).

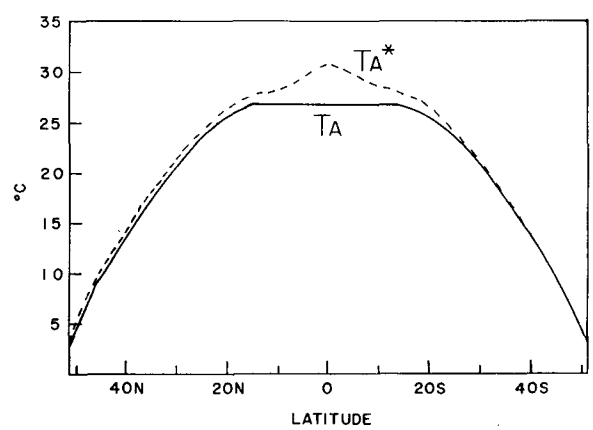

FIG. 11. The apparent atmospheric equilibrium temperature T_A^* computed from (35) using $C_D=1.4\times10^{-3}$ and the atmospheric equilibrium temperature T_A taken from Fig. 4.

using C_D from (30), the results do not differ significantly from those obtained using the constant value of C_D.

Eq. (34) gives the downward heat flux across the ocean surface in terms of the atmospheric equilibrium state which is specified by Q_2 and $T_A{}^*$, and the ocean surface temperature T_S which is not specified. In an ocean circulation model with a vertical structure like that in Fig. 1, the prediction equation for the temperature is applied at levels 1,2,$\cdots$ etc., but not at the surface. Thus, T_S must be defined in terms of the other dependent variables in the ocean model. In the absence of a satisfactory treatment of both the forced and free convective heat transport mechanisms which occur in the layer between the ocean surface and the first level below the surface, the most reasonable thing one can do is to assume that this sub-surface layer is always well mixed, and thereby replace T_S with T_1 in (34). This is the assumption used by Bryan (1969) and Manabe (1969) in the coupled stage of their ocean-atmosphere model. The downward heat flux across the ocean surface is then given by

$$Q=Q_2(T_A{}^*-T_1). \tag{36}$$

This formulation is shown schematically in Fig. 12.

Although the physical meaning of (36) is quite different from that expressed by (1), there is a definite similarity between the two. In both cases, the ocean temperature T_1 is coupled to an external temperature through a coupling factor. In (36), Q was derived in such a way that it represents the heat flux across the air-ocean interface, while in (1), Q represents the downward heat flux in the ocean between the surface and the depth Δz. However, when either formulation is used as a boundary condition on the temperature in an ocean circulation model, this distinction is lost, and T_1 is simply coupled to the specified external temperature. The first point to be emphasized from (36) is that the appropriate temperature to which T_1 should be coupled is not an ocean surface temperature T_S, nor an atmospheric temperature T_A, but rather an *apparent* atmospheric temperature $T_A{}^*$ (Fig. 11) which includes the effects of evaporation and solar radiation.

In (36), the coupling coefficient has been calculated from observed data using two slightly different profiles of the drag coefficient C_D. In (1), the coupling coefficient, $\kappa/\Delta z$, depends on the value assigned to the vertical eddy diffusion coefficient. Even though the appropriate value of C_D and its dependence on V_A may not be accurately known within a factor of 2, even less is known about the appropriate value of κ to be used in the uppermost layer of the ocean. The second point to be emphasized from (36) is that this formulation of coupling the ocean to the atmosphere avoids using the vertical eddy diffusion coefficient κ whose value is not well known in the surface layer.

Finally, it is important to note that the coupling coefficient in (36) is not simply a constant as it is in

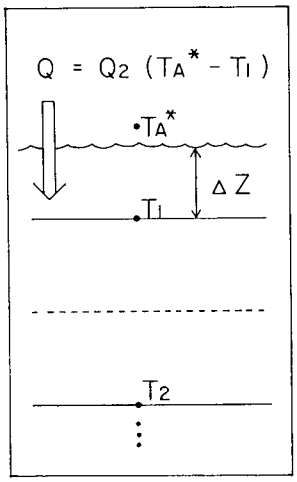

FIG. 12. Schematic diagram depicting the formulation of downward heat flux at the ocean surface according to (36). In this formulation the apparent atmospheric equilibrium temperature $T_A{}^*$ is prescribed.

(1), but that it is a function of latitude as shown in Figs. 8 and 9. The latitudinal variation of Q_2 reflects the fact that the heat transfer from the ocean to the atmosphere depends not only on the air-sea temperature difference, but also on some measure of the mean wind speed over the ocean. Because Q_2 helps determine the rate at which heat is taken up by the ocean in the tropics and given off to the atmosphere in high latitudes, it can affect the magnitude of the ocean's poleward heat transport. If C_D does increase with the strength of the wind roughly as indicated by (30), then we see in Fig. 9 that Q_2 is $\sim$20% larger in the high latitudes of the Southern Hemisphere than it is in the high latitudes of the Northern Hemisphere. This means that either the ocean temperatures will be more closely coupled to the atmosphere in the higher latitudes of the Southern as compared to the Northern Hemisphere, or else there will be a larger oceanic heat sink in the Southern Hemisphere. In a steady state, the latter situation would be accompanied by a larger oceanic poleward heat transport in the Southern Hemisphere than in the Northern Hemisphere.

This paper does *not* conclude that an ocean model which is driven by a prescribed, stationary atmospheric equilibrium state is preferable to a combined ocean-atmosphere model. Only with a combined and properly coupled ocean-atmosphere model can we study and understand the long-term interaction between the ocean and the atmosphere and such features as the partitioning of the poleward heat transport between the two.

Acknowledgments. The author wishes to thank Prof. Akio Arakawa and Dr. Kenzo Takano for their help and useful discussions on the subject of this work, and the editor and referees for their helpful comments and suggestions which contributed to an improved version of the final manuscript. The main part of this study

was done while the author was a graduate student at the University of California, Los Angeles, with support from the Atmospheric Sciences Section of the National Science Foundation, under Grant GA22756, and the U. S.-Japan Cooperative Science Program of the National Science Foundation, under Grant GF369. The final calculations and manuscript preparation was done under a grant from the Fleet Numerical Weather Facility.

REFERENCES

Brunt, D., 1952: *Physical and Dynamical Meteorology.*, Cambridge University Press, 428 pp.

Bryan, K., 1969: Climate and the ocean circulation III. The ocean model. *Mon. Wea. Rev.*, **97**, 806–827.

——, and M. D. Cox, 1967: A numerical investigation of the oceanic general circulation. *Tellus*, **19**, 54–80.

——, and——, 1968: A nonlinear model of an ocean driven by wind and differential heating: Part I. Description of the three-dimensional velocity and density fields. *J. Atmos. Sci.*, **25**, 945–967.

Budyko, M. I., N. A. Epinova, L. I. Zubenok and L. A. Strokina, 1962: The heat balance of the earth's surface. *Izv. Akad. Nauk SSSR, Ser. Geograf.*, **1**, 6–16.

Charney, J., 1959: On the general circulation of the atmosphere. *The Atmosphere and the Sea in Motion*, New York, Rockefeller Institute Press, 178–193.

Cox, M. D., 1970: A mathematical model of the Indian Ocean. *Deep-Sea Res.*, **17**, 47–75.

Deacon, E. L., and E. K. Webb, 1962: Interchange of properties between sea and air. *The Sea: Ideas and Observations*, Vol. 1, New York, Wiley (Interscience), 49–87.

Emig, M., 1967: Heat transport by ocean currents. *J. Geophys. Res.*, **72**, 2519–2529.

Fleagle, R. G., and J. A. Businger, 1963: *An Introduction to Atmospheric Physics*. New York, Academic Press, 346 pp.

Garstang, M., 1967: Sensible and latent heat exchange in low latitude synoptic scale systems. *Tellus*, **19**, 492–508.

Kasahara, A., and W. M. Washington, 1967: NCAR global general circulation model of the atmosphere. *Mon. Wea. Rev.*, **95**, 389–402.

Katayama, A., 1966: On the radiation budget of the troposphere over the Northern Hemisphere (I). *J. Meteor. Soc. Japan*, Ser. II, **44**, 381–401.

——, 1967: On the radiation budget of the troposphere over the Northern Hemisphere (II)—Hemispheric distribution. *J. Meteor. Soc. Japan*, Ser. II, **45**, 1–25.

Kraus, E. B., and C. Rooth, 1961: Temperature and steady state vertical heat flux in the ocean surface layers. *Tellus*, **13**, 231–238.

London, J., 1957: A study of the atmospheric heat balance. Final Rept., Proj. 131, Contract AF19 (122)-165, Dept. of Meteorology and Oceanography, NYU, 99 pp.

Malkus, J. S., 1962: Large-scale interactions. *The Sea: Ideas and Observations*, Vol. 1, New York, Wiley (Interscience), 88–294.

Manabe, S., 1969: Climate and the ocean circulation II. The atmospheric circulation and the effect of heat transfer by ocean currents. *Mon. Wea. Rev.* **97**, 775–805.

——, J. Smagorinsky and R. F. Strickler, 1965: Simulated climatology of a general circulation model with a hydrologic cycle. *Mon. Wea. Rev.*, **93**, 769–798.

Mintz, Y., 1964: Very long-term global integration of the primitive equations of atmospheric motion. *WMO/IUGG Symp. on Research and Development Aspects of Long-Range Forecasting*, Boulder, Colo., WMO Tech. Note No. **66**, 141–167.

Riehl, H., and J. S. Malkus, 1958: On the heat balance of the equatorial trough zone. *Geophysica (Helsinki)*, **6**, 503–538.

Sheppard, P. A., 1958: Transfer across the Earth's surface and through the air above. *Quart. J. Roy. Meteor. Soc.*, **84**, 205–224.

U. S. Naval Oceanographic Office, 1969: Monthly charts of mean, minimum, and maximum sea surface temperature of the North Pacific Ocean (SP-123). Naval Oceanographic Office, Washington, D. C. 20390, 62 pp.

U. S. Weather Bureau, 1938: *Atlas of Climatic Charts of the Oceans*. Washington, D. C., Govt. Printing Office, U. S. Weather Bureau No. 1247, 130 pp.

Vonder Haar, T. H., and K. J. Hanson, 1969: Absorption of solar radiation in tropical regions. *J. Atmos. Sci.*, **26**, 652–655.

Weiler, H., and R. W. Burling, 1967: Direct measurements of stress and spectra of turbulence in the boundary layer over the sea. *J. Atmos. Sci.*, **24**, 653–664.